

Research Article

Photovoltaic Water Pumping System Controlled by Cascade Sliding Mode

Rym Marouani, Mohamed Adel Sellami and Abdelkader Mami

Department of Physic, Faculty of Sciences of Tunis, Laboratory of Analyze, Conception and Control of Systems, National School of Engineering of Tunis, Tunisia

Abstract: This study presents a new maximum power point tracking algorithm applied to a photovoltaic water pumping system in order to optimize the photovoltaic power generation. This system is driven by an induction motor controlled by a cascade sliding mode control in order to track a set of reference trajectories such as currents, rotor flux and speed. By using the MATLAB-SIMULINK software, modeling and simulation studies are investigated to highlight the utility of the proposed system.

Keywords: Cascade sliding mode control, induction motor, maximum power point tracker, photovoltaic water pumping system

INTRODUCTION

In order to cover the energy requirement, researches are being made for renewable energy. Privately, Photovoltaic (PV) energy is produced by direct transformation of solar illumination to electrical energy. One of the world wide applications is the water pumping system driven by induction motor as it has been presented in Abid *et al.* (2007) and Mezouar *et al.* (2007).

In this study, the PV water pumping system is constituted by a PV generator, a condenser, a Pulse Width Modulation PWM inverter, an induction motor and a centrifugal pump.

In order to force the PV generator to operate at its maximum power point under different solar illumination values, we develop a maximum power point tracking algorithm MPPT which calculates the reference speed of the induction motor versus the solar illumination as in Abid *et al.* (2007), Arrouf and Bouguechal (2003) and Barazane *et al.* (2003). The induction motor is distinguished by its rigidity, reliability and relatively low cost. However, the difficulty to control the induction motor is related to the fact that its mathematical model in Park configuration is nonlinear and highly coupled as demonstrated in Arrouf and Ghabrou (2007), Mahmoudi *et al.* (1999), Marouani and Bacha (2009) and Tarik Duru (2007). Due to the development of power electronics and microprocessors, the induction motor control is possible by applying field oriented techniques as presented in Abid *et al.* (2007) and Mahmoudi *et al.* (1999).

These techniques provide the decoupling stator and rotor machine frames that allow obtaining a dynamical model similar to that of the direct current machine.

Nevertheless, a discontinuous behavior is imposed by the switching devices of the inverter supplying the induction machine. Therefore, it is suitable to look for some techniques which are appropriate to discontinuous operation of the switching devices. The Sliding Mode is an All or Nothing (AoN) control law which is the most appropriated to the control of the switchers of the power converters of the PV water pumping system. So, in this study, we will demonstrate that the Sliding Mode Control allows a high performance in controlling of the induction motor. Robustness of this control law will be highlighted versus changing parameters and external disturbances as it has been presented in Arrouf and Ghabrou (2007), Mimouni *et al.* (2004), Utkin (1993) and Weslati *et al.* (2008).

MODELING OF THE PHOTOVOLTAIC WATER PUMPING SYSTEM

The photovoltaic water pumping system includes a PV generator, a DC bus, an inverter, an induction motor and a centrifugal pump. Following sections present models of these subsystems.

The PVG model: The mathematic model of the PVG with N_s series connected solar cells and N_p parallel connected panels is given by (1), (Abid *et al.*, 2007; Arrouf and Bouguechal, 2003):

$$I_{pv} = N_p I_{ph} - N_p I_s \left[\exp\left(\frac{V_{pv} + R_s I_{pv}}{N_s V_T}\right) - 1 \right] - \left(\frac{V_{pv} + R_s I_{pv}}{R_{sh}} \right) \quad (1)$$

where,

Corresponding Author: Rym Marouani, Department of Physic, Faculty of Sciences of Tunis, Laboratory of Analyze, Conception and Control of Systems, National School of Engineering of Tunis, Tunisia

This work is licensed under a Creative Commons Attribution 4.0 International License (URL: <http://creativecommons.org/licenses/by/4.0/>).

I_{pv} , V_{pv} and P_{pv} = The Photovoltaic (PV) current, voltage and power
 I_{ph} = The light-generated current
 I_s = The reverse saturation current
 R_s and R_{sh} = The PV array series and shunt resistances
 A = The ideality factor
 K = The constant of Boltzman
 T = Cell temperature
 q = The electronic charge
 V_T = The thermodynamic potential $V_T = AKT/q$

$$R_{sm} = R_s + R_r M^2 / L_r^2$$

R_s and R_r = The stator and rotor resistances
 L_s and L_r = The stator and rotor inductances
 T_r = The rotor time constant ($T_r = L_r/R_r$)
 M = The mutual inductance
 ω_s = The stator angular frequency
 ω_r = The rotor speed
 σ = The total leakage coefficient ($\sigma = 1 - M^2/L_s L_r$)

The DC bus model: To avoid the submission of the PVG to the over-voltages coming from the inverter, we insert a condenser C between them. The DC bus current I_c is given by (2):

$$I_c = CdV_{pv} / dt \quad (2)$$

The inverter model: The three-phase inverter consists of three independent arms. Each one includes two switches which are complementary and controlled by the Pulse Width Modulation PWM as in Abid *et al.* (2007), Arrouf and Bouguechal (2003) and Arrouf and Ghabrou (2007). The stator voltages (v_{sa} , v_{sb} , v_{sc}) are expressed in terms of the upper switches as follows:

$$\begin{bmatrix} v_{sa} \\ v_{sb} \\ v_{sc} \end{bmatrix} = \frac{V_{pv}}{3} \begin{bmatrix} 2 & -1 & -1 \\ -1 & 2 & -1 \\ -1 & -1 & 2 \end{bmatrix} \begin{bmatrix} s_1 \\ s_2 \\ s_3 \end{bmatrix} \quad (3)$$

s_1 , s_2 and s_3 are the controller signals applied to the switches.

The induction motor model: By considering the stator voltages (v_{ds} , v_{qs}) as control inputs, the stator currents (i_{ds} , i_{qs}), the rotor flux (Φ_{dr} , Φ_{qr}) and the speed (Ω) as state variables, the electrical model of the induction motor in the d - q referential axis linked to rotating field is given by (7), as in Abid *et al.* (2007), Arrouf and Ghabrou (2007), Mahmoudi *et al.* (1999), Marouani and Bacha (2009) and Mezouar *et al.* (2007):

$$\begin{cases} \frac{di_{ds}}{dt} = \left(\frac{1}{sL_s}\right) \dot{\epsilon} R_{sm} i_{ds} + sL_s \omega_s i_{qs} + \left(\frac{M}{L_r}\right) \left(\frac{F_{dr}}{T_r}\right) + \omega_s F_{qr} + v_{ds} \dot{\eta} \\ \frac{di_{qs}}{dt} = \left(\frac{1}{sL_s}\right) \dot{\epsilon} R_{sm} i_{qs} - sL_s \omega_s i_{ds} + \left(\frac{M}{L_r}\right) \left(\frac{F_{qr}}{T_r}\right) - \omega_s F_{dr} + v_{qs} \dot{\eta} \\ \frac{dF_{dr}}{dt} = \left(\frac{M}{T_r}\right) i_{ds} + (\omega_s - \omega_r) F_{qr} - \frac{F_{dr}}{T_r} \\ \frac{dF_{qr}}{dt} = \left(\frac{M}{T_r}\right) i_{qs} - (\omega_s - \omega_r) F_{dr} - \frac{F_{qr}}{T_r} \end{cases} \quad (4)$$

where,

The mechanical modeling part of the system is given by:

$$Jd\Omega/dt = (C_{em} - C_r - f\Omega) \quad (5)$$

where,

J = The total inertia of the machine
 f = The coefficient of friction
 C_r = The load torque
 Ω = The mechanical speed of the machine

The electromagnetic torque is given by:

$$C_{em} = (3pM/2L_r) \cdot [\Phi_{dr} i_{qs} - \Phi_{qr} i_{ds}] \quad (6)$$

where, p is the number of pole pairs.

The hydrodynamic load torque of the centrifugal pump is given by (9) as in Abid *et al.* (2007):

$$C_r = A_p \omega_r^2 \quad (7)$$

where,

A_p = The torque constant ($A_p = P_n/\omega_{rn}^3$)
 P_n = The nominal power of the induction-motor
 ω_{rn} = The rotor nominal speed

The centrifugal pump model: The centrifugal pump is described by the laws of similarity which are given by (12) as in Marouani and Bacha (2009):

$$\begin{cases} Q' = (N'/N) \cdot Q \\ H' = (N'/N)^2 \cdot H \end{cases} \quad (8)$$

where, Q' and Q are, respectively the flow and the nominal flow of the pump, H' and H are, respectively his height and total height; N' and N are respectively his speed and nominal speed.

THE CASCADE SLIDING MODE CONTROL

The rotor flux field oriented control: By using the electrical model of the induction machine given by (6), one can remark the interaction of both inputs, which makes the control design more difficult. So, the first step of our work is to obtain a decoupled system in order to control the electromagnetic torque *via* the

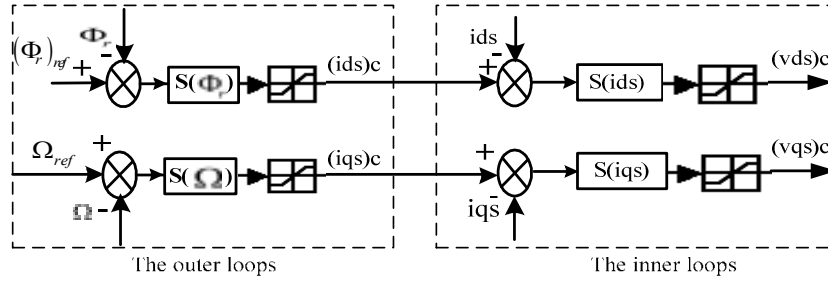


Fig. 1: The inner and outer loops of the SMC

stator quadrature current i_{qs} with a similar manner of a DC machine. The field orientation is obtained by (13) as in Mahmoudi *et al.* (1999), Marouani and Bacha (2009) and Tarik Duru (2007):

$$\begin{cases} \Phi_{dr} = \Phi_r \\ \Phi_{qr} = 0 \end{cases} \quad (9)$$

The rotor flux Φ_r and its position θ_s are estimated by means of stator current and speed and are given as follows:

$$\Phi_r = (M / (1 + sT_r))i_{ds} \quad (10)$$

$$\theta_s = \int ((M.i_{qs} / (T_r.\Phi_r)) + p\Omega)dt \quad (11)$$

where, s is the differential operator ($s = d/dt$).

Then, the stator equations on d, q -axis become, (Barazane *et al.*, 2003):

$$\begin{cases} \frac{di_{ds}}{dt} = \left(\frac{1}{\sigma L_s}\right) \left[v_{ds} - R_{sm}i_{ds} + \sigma L_s \omega_s i_{qs} + \left(\frac{M}{L_r T_r}\right) \Phi_r \right] \\ \frac{di_{qs}}{dt} = \left(\frac{1}{\sigma L_s}\right) \left[v_{qs} - R_{sm}i_{qs} - \sigma L_s \omega_s i_{ds} + \left(\frac{M}{L_r}\right) \omega_r \Phi_r \right] \end{cases} \quad (12)$$

Sliding mode control: In this study, the sliding mode control theory is applied to the rotor field oriented induction motor in such away to obtain simple surfaces. The proposed control scheme is a cascade structure as shown in Fig. 1, in which two surfaces for each axis are required. The internal loops allow to control the stator current components (i_{ds}, i_{qs}); whereas the external loops provide the speed and the rotor flux (Ω, Φ_r) regulations as in Arrouf and Ghabrou (2007) and Mimouni *et al.* (2004).

The sliding surfaces for each axis are chosen as follows:

$$d\text{-axis:} \begin{cases} S(\Phi_r) = (\Phi_r)_{ref} - \Phi_r \\ S(i_{ds}) = (i_{ds})_{ref} - i_{ds} \end{cases} \quad (13)$$

$$q\text{-axis:} \begin{cases} S(\Omega) = (\Omega)_{ref} - \Omega \\ S(i_{qs}) = (i_{qs})_{ref} - i_{qs} \end{cases} \quad (14)$$

The $(i_{ds})_{ref}$ and $(i_{qs})_{ref}$ references are determined by the outer loops and take, respectively the values of $(i_{ds})_c$ and $(i_{qs})_c$.

Using (13) and (14), it follows:

- On d -axis: for the rotor flux regulation, we have:

$$\dot{S}(\Phi_r) = 0 \Rightarrow (i_{ds})_{eq} = (\Phi_r + T_r \cdot \dot{\Phi}_{ref}) / M \quad (15)$$

$$\dot{S}(\Phi_r) \cdot S(\Phi_r) < 0 \Rightarrow (i_{ds})_n = \begin{cases} (k_\phi / \varepsilon_\phi) \cdot S(\Phi_r) & \text{if } |S(\Phi_r)| < \varepsilon_\phi \\ k_\phi \cdot \text{sgn}(S(\Phi_r)) & \text{if } |S(\Phi_r)| > \varepsilon_\phi \end{cases} \quad (16)$$

Thus, the controller is:

$$(i_{ds})_c = (i_{ds})_{eq} + (i_{ds})_n \quad (17)$$

And for direct current regulation, it follows:

$$\dot{S}(i_{ds}) = 0 \Rightarrow (v_{ds})_{eq} = \sigma L_s (i_{ds})_{ref} + R_{sm} i_{ds} - \sigma L_s \omega_s i_{qs} - (M / L_r T_r) \Phi_r \quad (18)$$

$$\dot{S}(i_{ds}) \cdot S(i_{ds}) < 0 \Rightarrow (v_{ds})_n = \begin{cases} (k_d / \varepsilon_d) \cdot S(i_{ds}) & \text{if } |S(i_{ds})| < \varepsilon_d \\ k_d \cdot \text{sgn}(S(i_{ds})) & \text{if } |S(i_{ds})| > \varepsilon_d \end{cases} \quad (19)$$

The controller on d -axis is given by:

$$(v_{ds})_c = (v_{ds})_{eq} + (v_{ds})_n \quad (20)$$

In the same way:

- On q -axis: for the speed regulation:

$$\dot{S}(\Omega) = 0 \Rightarrow (i_{qs})_{eq} = (J\dot{\Omega}_{ref} + k_f \Omega + C_r) / (pM\Phi_r / L_r) \quad (21)$$

$$\dot{S}(\Omega) \cdot S(\Omega) < 0 \Rightarrow (i_{qs})_n = \begin{cases} (k_\omega / \varepsilon_\omega) \cdot S(\Omega) & \text{if } |S(\Omega)| < \varepsilon_\omega \\ k_\omega \cdot \text{sgn}(S(\Omega)) & \text{if } |S(\Omega)| > \varepsilon_\omega \end{cases} \quad (22)$$

Table 1: Reference speed and PV power versus the illumination value

E (w/m ²)	P _{opt} (W)	Ω _{ref} (rad/sec)
50	60.15	51.54
100	132.90	67.14
150	210.50	78.26
200	299.00	87.97
250	385.80	95.77
300	473.00	102.50
350	561.10	108.50
400	654.90	114.25
450	748.00	119.42
500	841.00	124.18
550	934.90	128.64
600	1032.00	132.95
650	1129.00	136.99
700	1226.00	140.81
750	1324.00	144.46
800	1423.00	147.98
850	1523.00	151.37
900	1622.00	154.58
950	1723.00	157.72
1000	1825.00	160.77

And the controller is given by:

$$(i_{qs})_c = (i_{qs})_{eq} + (i_{qs})_n \quad (23)$$

And for the quadrature current regulation, it follows:

$$\dot{S}(i_{qs}) = 0 \Rightarrow (v_{qs})_{eq} = \sigma L_s (\dot{i}_{qs})_{ref} + R_{sm} i_{qs} + \sigma L_s \omega_s i_{ds} - (M/L_r) \omega_r \Phi_r \quad (24)$$

$$\dot{S}(i_{qs}) \cdot S(i_{qs}) < 0 \Rightarrow (v_{qs})_n = \begin{cases} (k_q / \varepsilon_q) \cdot S(i_{qs}) & \text{if } |S(i_{qs})| < \varepsilon_q \\ k_q \cdot \text{sgn}(S(i_{qs})) & \text{if } |S(i_{qs})| > \varepsilon_q \end{cases} \quad (25)$$

And the controller is given by:

$$(v_{qs})_c = (v_{qs})_{eq} + (v_{qs})_n \quad (26)$$

To satisfy the stability condition of the system, all of the following gains (k_d , k_q , k_Φ , k_Ω) should be chosen positive.

High performances must be obtained by choosing appropriate gains as in Arrouf and Ghabroul (2007). k_d and k_q take the admissible values of transient stator voltage in direct and quadrature axis, then $k_d = (v_{ds})_{\max}$ and $k_q = (v_{qs})_{\max}$. k_Φ takes the value of $(i_{ds})_{\max} = (\Phi_r)_{ref} / M$. k_Ω takes two times of stator quadrature current value $(i_{qs})_{\max}$ admissible by the machine.

Using Park transformation, the reference voltages in the (a, b, c) coordinates are given by (27) as in Abid *et al.* (2007):

$$\begin{bmatrix} (v_{sa})_c \\ (v_{sb})_c \\ (v_{sc})_c \end{bmatrix} = \sqrt{\frac{2}{3}} \begin{bmatrix} \cos(\theta_s) & -\sin(\theta_s) \\ \cos(\theta_s - \frac{2\pi}{3}) & -\sin(\theta_s - \frac{2\pi}{3}) \\ \cos(\theta_s + \frac{2\pi}{3}) & -\sin(\theta_s + \frac{2\pi}{3}) \end{bmatrix} \begin{bmatrix} (v_{ds})_c \\ (v_{qs})_c \end{bmatrix} \quad (27)$$

Calculation of the reference variables: The reference flux value is $(\Phi_r)_{ref} = 1 \text{ wb}$.

The reference speed Ω_{ref} is calculated by the MPPT algorithm analyzed in above section.

Maximum power point tracking algorithm: By neglecting frictions and losses, we can express the power of the induction motor as follows as in Abid *et al.* (2007):

$$P \approx C_r \Omega = A_p \Omega^3 \quad (28)$$

So, the reference speed Ω_{ref} can be expressed as:

$$\Omega_{ref} = \sqrt[3]{P_{opt} / A_p} \quad (29)$$

Table 1 presents the reference speed and the optimal PV power for different values of the solar illumination.

We can determinate the relation between illumination E and the approximated reference speed Ω_{app}^* by using the curve fitting technique as in Abid *et al.* (2007), Arrouf and Bouguechal (2003) and Barazane *et al.* (2003). The approximated reference speed is given by (30):

$$\Omega_{mpp}^* = 36.325 + 0.3511 \cdot E - 5.795 \cdot 10^{-4} \cdot E^2 + 5.611 \cdot 10^{-7} \cdot E^3 - 2.088 \cdot 10^{-10} \cdot E^4 \quad (30)$$

Architecture of the photovoltaic water pumping system: The architecture of the photovoltaic water pumping system is described by Fig. 2. The subsystems of the proposed configuration are a PV generator, a condenser, a PWM inverter, an induction-motor and a centrifugal pump.

The main components of the sliding mode control block are the four sliding surfaces $S(\Phi_r)$, $S(\Omega)$, $S(i_{ds})$ and $S(i_{qs})$. In order to calculate the reference speed, we use a sensor to measure the illumination value and a calculator to deduce the reference speed *via* the MPPT.

RESULTS AND DISCUSSION

In order to demonstrate the effectiveness of the proposed control technique applied to the photovoltaic water pumping system, some simulations have been carried out. So, the proposed design scheme which is described by Fig. 2 is implemented in MATLAB/SIMULINK software using parameters given in Table 2.

Variation of the solar illumination value E: In a first step, we choose to vary the solar illumination value E as it is shown in Fig. 3 and to see its impact on the performances of the photovoltaic water pumping.

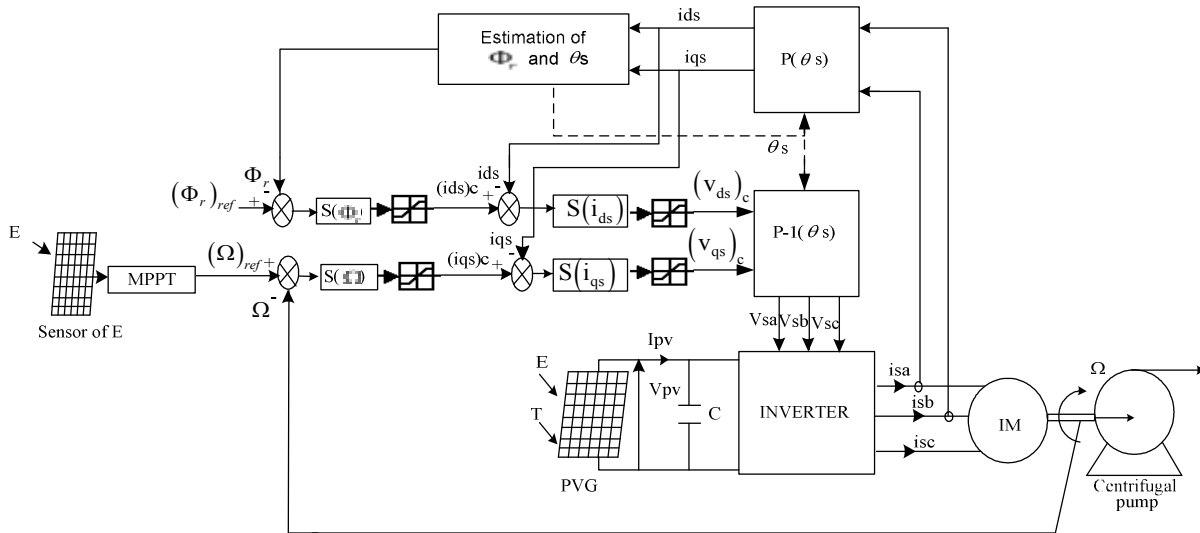


Fig. 2: Architecture of the photovoltaic water pumping system controlled by the sliding mode control

Table 2: PV generator parameters

PV generator parameters	
$P_{pv} = 50$ (Wc)	$V_{pv} = 17, 2$ (V)
$I_{pv} = 2.9$ (A)	$N_s = 36$
$N_p = 36$	$C = 2000$ (μ F)
Induction motor parameters	
$R_s = 5.72$ (Ω)	$R_r = 4.2$ (Ω)
$L_s = L_r = 0.462$ (H)	$M = 0.44$ (H)
$J = 0.0049$ ($Kg.m^2$)	$f = 1.5.10^{-4}$ (Nm/rds^{-1})
$p = 2$ pole pairs	$P = 1.5$ (Kw)
Centrifugal pump parameters	
$Q = 15$ (m^3/h)	$H = 20$ (m)
$N = 1450$ (tr/min)	

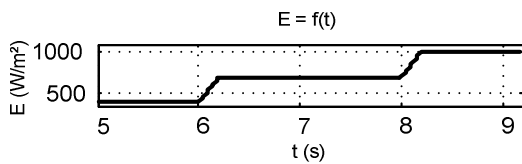


Fig. 3: The solar illumination waveform

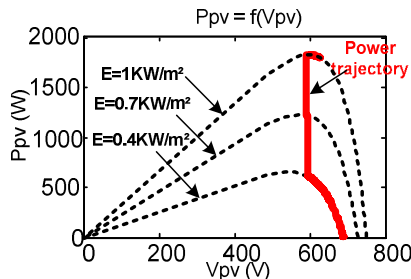


Fig. 4: Trajectories of the PV power for different value of solar illumination

Figure 4 shows, respectively the trajectory of the PV Power and PV current versus PV voltage. One can remark that at the moments of change of E, the PV curves are adjusted to their new optimal values

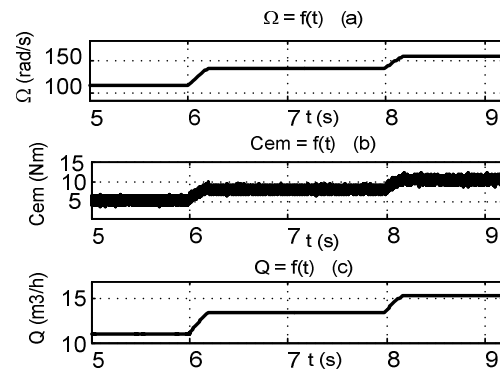


Fig. 5: Simulation results for the SMC under illumination variation

corresponding to the new value of E after a short transient.

So, we can note the utility of the MPPT algorithm in optimization of the PVG performances.

Figure 5a illustrates the waveform of the mechanical speed of the induction motor which is closed to its optimal value.

The same remark is given to the electromagnetic torque shown by Fig. 5b.

It is clearly shown that the induction motor is operating at its optimal conditions. Figure 5c represents the waveform of the centrifugal pump flow which is closed to its optimal value for each value of E.

Then, we can conclude the important role of the sliding mode control and the proposed MPPT to make the photovoltaic water pumping system operating at its optimal conditions.

Study of the robustness of the system: In a second step, we choose to vary the rotor time constant T_r

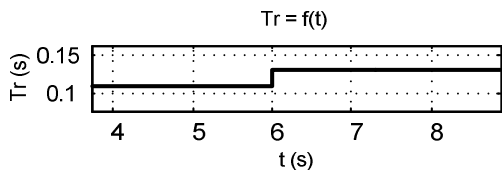


Fig. 6: The variation of the rotor time constant

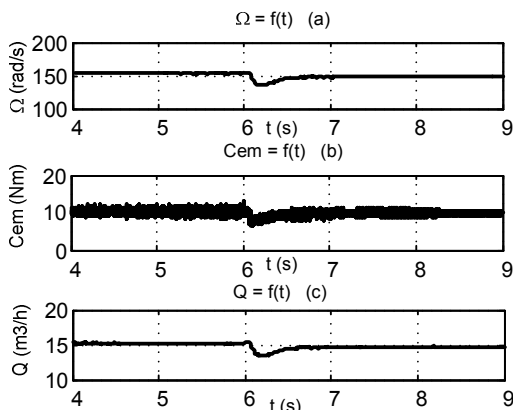


Fig. 7: Simulation results for the SMC with parameters variation

at 20% of its initial value at it is shown in Fig. 6, in order to prove the robustness of the system at the disturbances and the drifts of the motor driven pump parameters.

Figure 7a to c show, respectively the waveform of the motor speed, the electromagnetic torque and the pump flow.

So, a rapid response is obtained. The different variables are lightly affected by the T_r change at a short transient and then, they return to their optimal values. The same remark is given to the centrifugal pump flow which proves that the water pumping system operating at its optimal conditions.

Then, the robustness of the controlled system is highlighted by the appropriate type controller which is a sliding mode control and the cascade structure used.

CONCLUSION

We have proved the utility of the developed algorithm MPPT in resolution of the problem of degradation of the performances of the PV generator following the variation of the power according to climatic factors and its role to minimize the total cost since it replaces electronic devices like converter used for tracking of the maximum power point.

Furthermore, the sliding mode control applied to the field oriented induction motor pump has succeeded in the regulation of the motor speed and then in optimization of the performances of the system. Such a control scheme provides protection of the connected inverter and machine with regards to stator current

since these latter are controlled. Besides, the robustness quality of the proposed controllers appears clearly in the test results by changing machine parameters. Finally, this installation provides the minimization of the total cost since we choose to stock the water and not the energy which requires the use of electrical batteries.

REFERENCES

- Abid, M., A.G. Aissaoui, Y. Ramdani and A.K. Zeblah, 2007. Sliding mode speed and flux control of field-oriented induction machine. *Acta Electrotechnica et Informatica*, 7: 1-7.
- Arrouf, M. and N. Bouguechal, 2003. Vector control of an induction motor fed by a photovoltaic generator. *Appl. Energ.*, 74: 159-167.
- Arrouf, M. and S. Ghabrou, 2007. Modelling and simulation of a pumping system fed by photovoltaic generator within the Matlab/Simulink programming environment. *Desalination*, 209: 23-30.
- Barazane, L., Y. Sellami, R. Ouiguini and M.S. Boucherit, 2003. An approach to cascade sliding mode control of an induction motor based on robust neural network controllers. *Proceeding of the International Conference on Telecommunication Systems, Medical Electronic and Automatism*.
- Mahmoudi, M.O., N. Madani, M.F. Benkhoris and F. Boudjema, 1999. Cascade sliding mode control of a field oriented induction machine drive. *Eur. Phys. J-Appl. Phys.*, 7: 217-225.
- Marouani, R. and F. Bacha, 2009. A maximum-power-point tracking algorithm applied to a photovoltaic water-pumping system. *Proceeding of the 8th International Symposium on Advanced Electromechanical Motion Systems and Electric Drives Joint Symposium*.
- Mezouar, A., M.K. Fellah and S. Hadjeri, 2007. Adaptive sliding mode observer for induction motor using two-time-scale approach. *Electr. Pow. Syst. Res.*, 77: 604-618.
- Mimouni, M.F., M.N. Mansouri, B. Belgacem and M. Annabi, 2004. Vectorial command of an asynchronous motor fed by a photovoltaic generator. *Renew. Energ.*, 29: 433-442.
- Tarik Duru, H., 2007. A maximum power tracking algorithm based on $I_{mpp}=f(P_{max})$ function for matching passive and active loads to a photovoltaic generator. *Sol. Energy*, 80: 812-822.
- Utkin, V.I., 1993. Sliding mode control design principles and applications to electric drives. *IEEE T. Ind. Electron.*, 40: 23-36.
- Weslati, Y., A. Sellami, F. Bacha and R. Andoulsi, 2008. Sliding mode control of a photovoltaic grid connected system. *J. Electr. Syst.*, 4: 1-14.